A Study of Reversible γ-Induced Structural Transformations in Vitreous $Ge_{23.5}Sb_{11.8}S_{64.7}$ by High-Resolution X-ray Photoelectron Spectroscopy

Andriy Kovalskiy,[†] Himanshu Jain,*[,†] Alfred C. Miller,[†] Roman Ya. Golovchak,[†,‡] and Oleh I. Shpotyuk[†,‡,§]

Department of Materials Science and Engineering, Lehigh University, 5 East Packer Avenue, Bethlehem, Pennsylvania 18015-3195, Lviv Scientific Research Institute of Materials of SRC "Carat", 202 Stryjska str., Lviv, UA-79031, Ukraine, and Institute of Physics of Jan Dlugosz University, 13/15, al. Armii Krajowej, Czestochowa, PL-42201, Poland

Received: May 11, 2006; In Final Form: August 30, 2006

The structural origin of reversible γ-induced effects in vitreous $Ge_{23.5}Sb_{11.8}S_{64.7}$ has been investigated by high-resolution X-ray photoelectron spectroscopy (XPS). The changes in valence band spectrum from γ-irradiation suggest a decrease of sulfur lone pair electron concentration accompanied by changes in bonding states of S and Ge. The appearance of additional doublets in the core-level XPS spectra of Ge, Sb, and S atoms for γ-irradiated sample is described by the formation of over- and under-coordinated charged defect pairs ($Ge_3^- - S_3^+$) as a result of radiation treatment. The results verify the switching of Ge−S covalent bonds into S−S bonds as the main microstructural mechanism for γ-induced optical effects in this glass.

Introduction

Chalcogenide glasses (ChG) are known to be sensitive to high-energy ionizing radiation such as γ-rays, accelerated electrons, deuterons, etc.[1−4] Of particular interest are γ-induced effects that can be utilized for industrial dosimetry[4,5] and modification of ChG properties.[6] Recently, it was shown that these effects are caused by a so-called destruction−polymerization transformation involving switching of covalent chemical bonds and a simultaneous formation of coordination topological defects (pairs of under- and over-coordinated atoms).[7] Because of strong electron−phonon coupling in ChG,[8] these processes depend on the changes in the atomic as well as the electronic structure. So far little attention has been given to the changes in the electronic structure by high-energy irradiation. Therefore, in the present work, γ-induced changes in the valence band, as well as in the core electron levels of vitreous v-$Ge_{23.5}Sb_{11.8}S_{64.7}$, are investigated by high-resolution X-ray photoelectron spectroscopy (XPS). Previously, this method was applied effectively to understand the effects induced in the thin films of ChG by band gap light.[9−11]

The v-$Ge_{23.5}Sb_{11.8}S_{64.7}$ composition was selected as a representative of the GeS_2-Sb_2S_3 family, which appears to show relatively simple radiation-induced structural transformations. Only one bond-switching scheme has been attributed to explain the observed γ-induced optical changes in this glass.[7] So, compared to vitreous arsenic and mixed arsenic−germanium sulfides that show complicated bond-switching schemes, sometimes even of opposite character,[1,2] we expect model results to help understand the fundamental nature of high-energy radiation effects in v-$Ge_{23.5}Sb_{11.8}S_{64.7}$.

* Address correspondence to this author: Phone: 1-610-758-4217. E-mail: h.jain@lehigh.edu.
[†] Lehigh University.
[‡] Lviv Scientific Research Institute of Materials of SRC "Carat".
[§] Institute of Physics of Jan Dlugosz University.

Experimental Methods

Bulk v-$Ge_{23.5}Sb_{11.8}S_{64.7}$ samples were prepared by melting the mixture of high-purity (99.999%) Ge, Sb, and S powders sealed in an evacuated (10^{-3} Pa) quartz ampule. The furnace was rocked for 24 h to obtain a homogeneous melt. Then the melt was cast by quenching to ambient temperature and annealed near T_g (623 K) to remove residual mechanical stresses introduced from nonuniform cooling. The amorphous state of the prepared ChG was verified by observing a characteristic conch-like fracture, as well as from X-ray diffraction analysis and IR transmission microscopy.

To exclude the irreversible component of structural changes that occur only the first time when an as-prepared ChG sample is exposed to γ-irradiation,[12] the investigated samples were subjected to a preliminary treatment in the first cycle consisting of γ-irradiation and annealing near T_g. Then the samples were treated to the second fully reversible cycle, which included γ-irradiation with an accumulated dose of 7.7 MGy and a subsequent thermal annealing.

The samples were irradiated in a closed cylindrical cavity of concentrically maintained ^{60}Co sources (the so-called stationary radiation field conditions) with a few Gy/s dose rate and temperature not exceeding ~310 K. Some of the γ-irradiated samples were thermally annealed at T_g in a vacuum for 4 h. Both the γ-irradiated and thermally annealed v-$Ge_{23.5}Sb_{11.8}S_{64.7}$ samples were used for XPS measurements.

The XPS spectra were recorded with Scienta ESCA-300 spectrometer with a monochromatic Al Kα X-ray (1486.6 eV) spot that was ~3−4 mm long and ~250 μm wide. Data acquisition was restricted electronically to a smaller region within the X-ray illuminated area. For all measurements the angle between the surface and the detector was 90° with a depth of analysis of ~100 Å. The instrument was operated in a mode that yielded a Fermi-level width of 0.4 eV for Ag metal. The residual pressure inside the analysis chamber was better than 10^{-8} Torr. To eliminate surface contamination from reaction with the atmosphere, the bulk ChG sample was fractured with

10.1021/jp062900t CCC: $33.50
Published on Web 10/12/2006

a hard tool in the ultrahigh vacuum inside the spectrometer. The energy scale was calibrated by using the Fermi level of clean Ag.

The XPS data consisted of survey scans over the entire binding energy range, and selected scans over the valence band or core-level photoelectron peaks of interest. An energy increment of 1.0 eV was used for recording the survey spectra and 0.05 eV for the case of core-level spectra. The core-level peaks were recorded by sweeping the retarding field and using the constant pass energy of 150 eV. Reproducibility of the measurements was confirmed on different regions of fractured surfaces of a sample, as well as on different γ-irradiated and annealed samples. The surface charging from photoelectron emission was neutralized by using a low-energy (<10 eV) electron flood gun, which minimized any distortion and shift of spectra. To accommodate differences in surface potentials between specimens, the raw spectra were shifted such that the midpoint of the steep rise of the top edge of the valence bands coincided with the zero of binding energy. Data analysis was conducted with a standard ESCA-300 software package. For analyzing the core-level spectra, Shirley background was subtracted and a Voigt line-shape was assumed for the peaks.[13] Concentrations of appropriate chemical elements were determined from the area of core-level peaks taking into account appropriate sensitivity coefficients.

Each core-level spectrum was fitted to obtain sets of doublets representing the spin−orbit splitting of d and p electron core levels. The number of doublets within a given peak was determined by the goodness of fitting. Only those doublets were considered which significantly improved the goodness of fitting. Splitting parameters (intensity ratio and peak separation) for the doublets of a particular element were chosen from the measurements of standard spectra of pure Ge, Sb, and S elements and their stoichiometric compounds under similar spectrometer settings. The full width at half-maximum (fwhm) was assumed to be the same for the peaks within one doublet. However, different fwhm values were allowed for independent doublets of the same core-level peak. The mix between the Gaussian and Lorentzian in the Voigt function was chosen the same for all doublets of a given core-level. The fitting procedure gave mix values close to 90% Gaussian and 10% Lorentzian and asymmetry values close to zero for all peaks. With these constraints the uncertainty in peak position and area of each component was ±0.05 eV and ±2%, respectively.

For comparing the valence band intensity of different samples, the spectra were scaled such that their intensity was the same at binding energies >20 eV, where we expect little change in the deep bonding states.

Results and Discussion

It was shown previously that γ-irradiation of v-$Ge_{23.5}Sb_{11.8}S_{64.7}$,[6,12] just like that of many other S-containing ChG,[1,2] causes darkening via a red (long-wave) shift of fundamental optical absorption edge with a simultaneous decrease in its slope. This effect can be erased simply by thermal annealing of γ-irradiated sample near T_g, revealing both irreversible and reversible components of the structural change.[12] The irreversible component is observed only during the first γ-irradiation/thermal annealing cycle; subsequent γ-irradiation produces fully reversible changes in the fundamental optical absorption edge region.[14]

The origin of reversible γ-induced optical effects in ChG was connected with the formation of specific topological coordination defects, viz., pairs of over-coordinated positively-charged and under-coordinated negatively-charged atoms.[14] Due to the

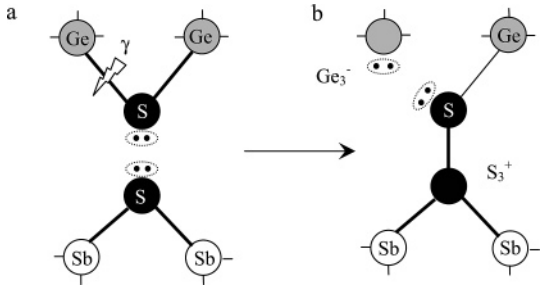

Figure 1. Coordination defects in stoichiometric v-Sb_2S_3-GeS_2 produced by switching of heteroatomic Ge−S covalent bonds into homoatomic S−S ones: (a) initial state and (b) final state (the lone pair of electrons are indicated by dotted ellipses).

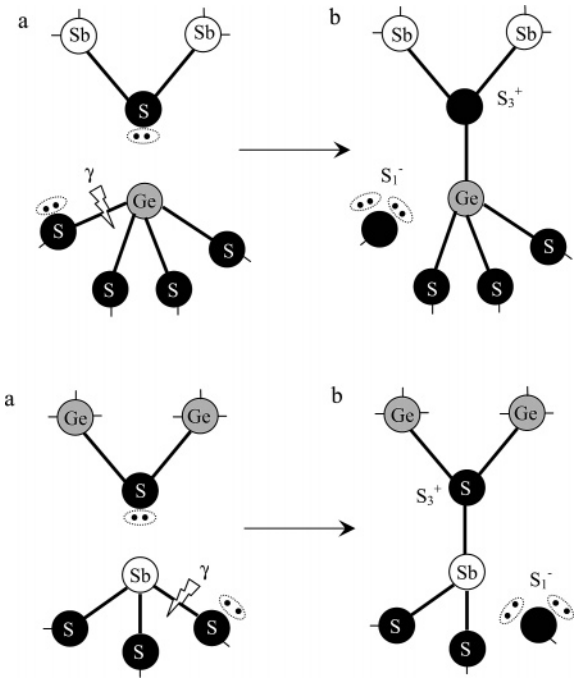

Figure 2. Coordination defects in stoichiometric v-Sb_2S_3-GeS_2 produced by bond-type-conserving switching of heteroatomic Ge−S (the upper scheme) and Sb−S (the lower scheme) covalent bonds: (a) initial state and (b) final state (the lone pair of electrons are indicated by dotted ellipses).

significant metallic nature of the covalent bonding of Sb atoms, Sb-based coordination defects were not considered important. Using a topological mathematical modeling procedure described elsewhere,[7] the Ge_3^- and S_3^+ defect pairs (the subscript designates the local coordination of the atom, and the superscript indicates its excess electrical charge) were assumed as the main defects responsible for γ-induced optical effects in v-$Ge_{23.5}Sb_{11.8}S_{64.7}$. The topological scheme of this defect-formation process is shown in Figure 1. Such coordination defects may appear in a glass network as a result of switching of heteroatomic Ge−S covalent bonds into "wrong" homoatomic S−S bonds induced by γ-irradiation. Thus, the observed γ-induced red shift of the fundamental optical absorption edge in v-$Ge_{23.5}Sb_{11.8}S_{64.7}$ was explained by the increase in the covalent bonding disorder that is initially introduced during freezing of melt near T_g. The decrease of slope in the fundamental optical absorption edge was associated with additional local deviations in electrical fields of randomly distributed coordination defects.[15]

In addition, two other γ-induced bond-switching schemes occurring without change in the bond type and, consequently, without change in average energy of covalent bonding are possible in v-$Ge_{23.5}Sb_{11.8}S_{64.7}$ (see Figure 2). As indicated by

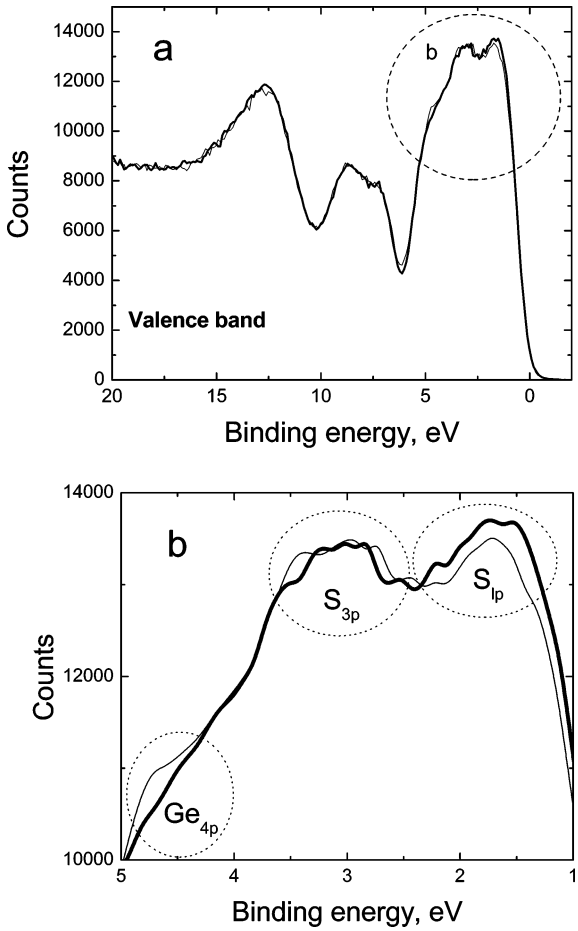

Figure 3. XPS valence-band spectra of γ-irradiated (thin curve) and nonirradiated (bold curve) v-$Ge_{23.5}Sb_{11.8}S_{64.7}$ (a) and enlarged fragment (b) showing (dotted circles) the most significant changes.

topological-mathematical modeling,[7] both schemes result in homoatomic ($S_3^+-S_1^-$) defect pairs, which increase disorder in the intrinsic electrical field with a corresponding decrease in the slope of the fundamental optical absorption edge.[15] However, the probability of such structural transformations is low because of the small difference in the dissociation energies of switched covalent bonds.[7] The backward defect-eliminating transformations would be fast in this case even at relatively low room temperatures.

It should be noted that here we have considered radiation-induced coordination topological defects, but not the natural defects frozen during initial quenching near the glass transition temperature. For the latter case, the concentration is very small ($10^{17}-10^{18}$ cm^{-3}),[16] while for the former case it can reach even 10^{20} cm^{-3} (or 6−8% of the total concentration of atoms within the glass network), causing significant changes in the glass properties.[1,7] Thus, a significant effect on the electronic subsystem of γ-irradiated v-$Ge_{23.5}Sb_{11.8}S_{64.7}$ may arise from the "wrong" homoatomic S−S covalent chemical bonds and randomly distributed pairs of charged ($Ge_3^--S_3^+$) coordination defects.

The valence-band XPS spectra of γ-irradiated and thermally annealed v-$Ge_{23.5}Sb_{11.8}S_{64.7}$ are shown in Figure 3. The irradiation decreases the intensity of the band at a binding energy of ~1.7 eV, which is associated with the lone pair (lp) electrons of S.[17,18] In addition, γ-irradiation increases the XPS signal at ~4−5 eV that is connected with the 4p electrons of Ge, and causes significant broadening of the peak centered at 3 eV due to the 3p electrons of S bonding states.[17−20]

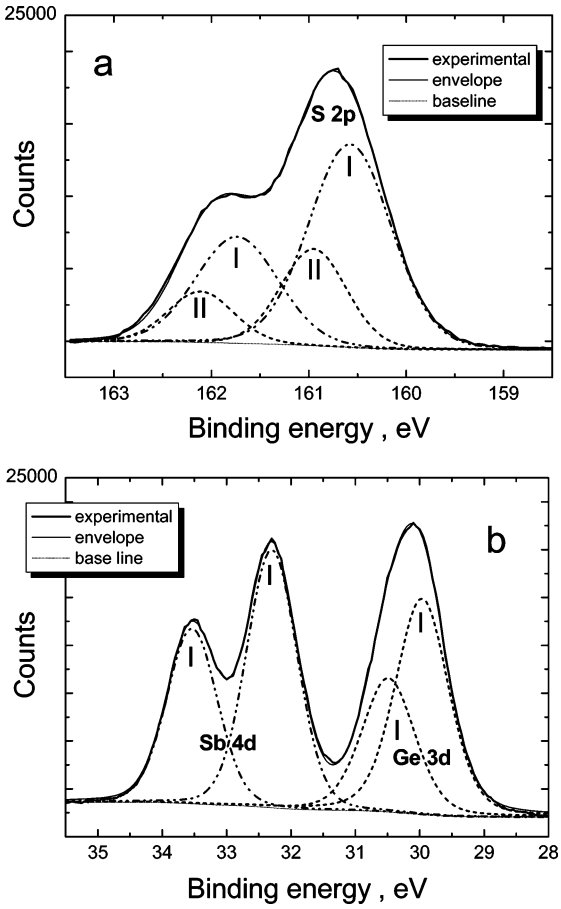

Figure 4. XPS core-level spectra of nonirradiated v-$Ge_{23.5}Sb_{11.8}S_{64.7}$: S 2p (a) and Ge 3d and Sb 4d (b).

The broadening of the peak at ~3 eV is expected as a result of new S-based covalent bonds formed within the glass network after γ-irradiation. Its main source appears to be homoatomic S−S covalent bonds linked with S_3^+ defects. The excess positive electrical charge on S_3^+ defects disturbs the bonding states of these overcoordinated atoms and leads to additional widening of the above peak. As such, we should expect a decrease in the intensity of the 3 eV electron band due to S−Ge covalent bonds according to the bond switching reaction shown in Figure 1. Apparently, it is not resolved because of the overlapping of four peaks of S-based bonds (S−Ge, S−Sb, S−S_3^+, S_3^+−Sb). If we accept the possibility of homoatomic ($S_3^+-S_1^-$) defect pair formation according to bond-conserving switching shown in Figure 2, the contribution to the 3 eV peak is expected also from S_3^+ and S_1^- defects neighboring the Sb and Ge atoms (S_3^+−Ge, S_3^+−Sb, S_1^-−Ge, S_1^-−Sb).

The existence of Ge_3^- defects in γ-irradiated ChG is supported by the increase of XPS signal in the region of ~4−5 eV due to Ge 4p electrons of the additional lone pair (see Figure 1). This assignment is in good agreement with the density of states calculations for amorphous GeS_2[19,21,22] and $GeSe_2$[17,23,24] and experimental results obtained for GeS_2.[18]

More detailed information on the above processes in v-$Ge_{23.5}Sb_{11.8}S_{64.7}$ caused by γ-irradiation can be obtained by analyzing core-level XPS spectra. Figure 4a shows an S 2p core-level XPS spectrum for thermally annealed ChG. This spectrum cannot be fitted by just one pair of spin−orbit split $2p_{3/2}$ and $2p_{1/2}$ peaks (doublets). It requires at least two doublets: the first pair marked I in the figure is attributed to regular S atoms within $GeS_{4/2}$ tetrahedra (S_{Ge} sites), and the other one marked II is attributed to $SbS_{3/2}$ pyramids (regular S_{Sb} sites). In principle, the S sites

TABLE 1: Numerical Parameters of XPS Core-level S 2p Spectra for Non-irradiated and γ-irradiated v-$Ge_{23.5}Sb_{11.8}S_{64.7}$

	core-level peak											
	S $2p_{3/2}$-I (S_{Ge}-reg)			S $2p_{3/2}$-II (S_{Sb}-reg)			S $2p_{3/2}$-III (S_S-CTD)			S $2p_{3/2}$-IV (S_S-irreg)		
sample	area, %	position, eV	fwhm	area, %	position, eV	fwhm	area, %	position, eV	fwhm	area, %	position, eV	fwhm
nonirradiated	73	160.55	0.98	27	160.95	0.78						
γ-irradiated	69	160.50	0.92	25	160.90	0.82	3	160.05	0.70	3	161.35	1.20

TABLE 2: Numerical Parameters of XPS Core-Level Sb 4d Spectra for Nonirradiated and γ-Irradiated v-$Ge_{23.5}Sb_{11.8}S_{64.7}$

	core-level peak					
	Sb $4d_{5/2}$-I (Sb_S-reg)			Sb $4d_{5/2}$-II (Sb_S-irreg)		
sample	area, %	position, eV	fwhm	area, %	position, eV	fwhm
nonirradiated	100	32.30	0.92			
γ-irradiated	95	32.15	0.93	5	33.05	1.20

TABLE 3: Numerical Parameters of XPS Core-Level Ge 3d Spectra for Nonirradiated and γ-Irradiated v-$Ge_{23.5}Sb_{11.8}S_{64.7}$

	core-level peak					
	Ge $3d_{5/2}$-I (Ge_S-reg)			Ge $3d_{5/2}$-II (Ge_S-CTD)		
sample	area, %	position, eV	fwhm	area, %	position, eV	fwhm
nonirradiated	100	29.95	0.94			
γ-irradiated	94	29.85	1.02	6	29.70	0.46

neighboring with both $SbS_{3/2}$ pyramids and $GeS_{4/2}$ tetrahedra could result in another separate doublet between the former two sets, but it could not be resolved in the spectra of investigated samples due to their very similar binding energies. There are no other additional distinct components in the fitted core-level spectra, testifying to stoichiometric uniformity in the environment of S atoms in thermally annealed v-$Ge_{23.5}Sb_{11.8}S_{64.7}$, i.e., there are no observable homoatomic bonds in the annealed sample. The characteristics of the S core-level peaks are given in Table 1. They are in good agreement with the analogous values given by other authors[18,25,26] (the somewhat higher values of binding energies from present data are most likely due to the difference in reference energy). The ratio of the areas of S $2p_{3/2}$-I and S $2p_{3/2}$-II peaks (73:27, see Table 1) is in excellent agreement with the nominal chemical composition expected from the chemical formula v-$Ge_{23.5}Sb_{11.8}S_{64.7}$. The peaks attributed to S atoms within $SbS_{3/2}$ pyramids appear at higher binding energy (160.95 eV for the $2p_{3/2}$-II peak), compared to the peaks due to S atoms within the $GeS_{4/2}$ tetrahedra (160.55 eV for $2p_{3/2}$-I peak). This difference in peak energies is easily understood from the difference in electronegativity χ of S, Sb, and Ge atoms, viz., 2.58, 2.05, and 2.01, respectively.[27] The $\Delta\chi$ value is higher for the Ge−S bond in comparison to that for the Sb−S pair, leading to a more effective charge transfer to S atoms in Ge−S than in Sb−S bonds.[25]

Figure 4b represents Sb 4d and Ge 3d core-level XPS spectra of thermally annealed v-$Ge_{23.5}Sb_{11.8}S_{64.7}$, identified as 4d-I and 3d-I doublets, corresponding to regular Sb atoms within $SbS_{3/2}$ pyramids and regular Ge atoms within $GeS_{4/2}$ tetrahedra, respectively (Tables 2 and 3). The distance between the above peaks is 2.35 eV in good agreement with the analogous data for thin Ge−Sb−S films.[27−29] As expected, no additional components appear in the spectrum due to structural uniformity of thermally annealed samples, which contrasts with earlier reports claiming the absence of the Ge 3d peak due to Ge atoms within $GeS_{4/2}$ tetrahedra.[29,30]

The S 2p, Sb 4d, and Ge 3d core-level spectra for thermally annealed and γ-irradiated v-$Ge_{23.5}Sb_{11.8}S_{64.7}$ samples are compared in parts a and b of Figure 5. Additional components are required for the satisfactory fitting of spectra obtained for all three elements after irradiation. The corresponding numerical parameters for peaks fitted from these spectra are given in Tables 1−3. The S 2p XPS spectrum shows a small decrease (∼4%) in the S $2p_{3/2}$-I peak, responsible for regular S_{Ge} sites within $GeS_{4/2}$ tetrahedra, along with a similar (∼2%) decrease in the S $2p_{3/2}$-II peak responsible for regular S_{Sb} sites within $SbS_{3/2}$ pyramids (see Figure 5a and Table 1). Both changes are in good agreement with the coordination defects formation scheme in Figure 1. The destruction of Ge−S bonds reduces the first S 2p peak, while S_3^+ defects next to Sb atoms cause a decrease in the other peak. At the same time, two additional weak doublets with main components, $2p_{3/2}$-III and $2p_{3/2}$-IV, of approximately the same intensity ∼3% appear in the S 2p core-level spectrum (see Table 1). The first doublet can be attributed to S_3^+ defects surrounded by two Sb and one S atoms, as shown in Figure 1. The second doublet can be associated with irregular S_S sites representing 2-fold coordinated S atom neighboring with Ge atom and S_3^+ coordination defect. Because of charge transfer toward S_3^+ defect within irregular S_S sites, the binding energy of the S $2p_{3/2}$-IV peak is sufficiently increased (161.35 eV) with respect to that of regular S_{Ge} sites (160.50 eV). This is also the reason for the lowest binding energy for the S $2p_{3/2}$-III peak (160.05 eV) associated with S_3^+ defect sites.

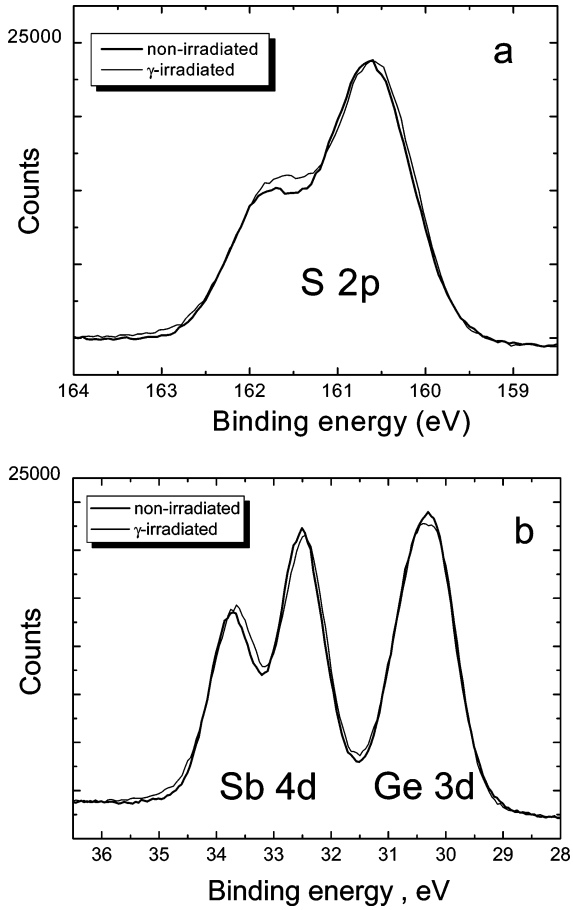

Figure 5. A comparison of XPS core-level S 2p (a) and Ge 3d and Sb 4d (b) spectra for nonirradiated and γ-irradiated v-$Ge_{23.5}Sb_{11.8}S_{64.7}$.

The γ-induced destruction of the network shown in Figure 1 causes corresponding changes in Sb 4d and Ge 3d core-level spectra too (see Figure 5b and Tables 2 and 3). An acceptable analysis of Sb and Ge core levels is not possible without introducing additional doublets for the γ-irradiated sample. The Sb $4d_{5/2}$-II component ($\sim$5% intensity, Table 2) arises from Sb$-S_3^+$ sites as a result of the S_3^+ positive charge influence on the electronic density of the Sb$-$S covalent bond. So, it is quite reasonable that its binding energy at 33.05 eV is 0.9 eV greater than that of the Sb $4d_{5/2}$-I peak. The observed decrease in the intensity of Sb $4d_{5/2}$-I peaks also follows the scheme of Figure 1 where Sb$-$S regular bonds should decrease after γ-irradiation. The Ge $3d_{5/2}$-II component ($\sim$6%, Table 3) is attributed to Ge_3^- defects. Its position is slightly shifted by $\sim$0.15 eV toward lower binding energies in comparison to the Ge $3d_{5/2}$-I peak because of higher electron density on Ge_3^- defect.

The relatively small differences in peak positions for the thermally annealed vs γ-irradiated ChG suggest that no significant phase separation occurs due to γ-irradiation. Also the chemical composition for γ-irradiated sample remains unchanged within the experimental error.

Conclusions

Reversible γ-induced structural transformations in v-$Ge_{23.5}Sb_{11.8}S_{64.7}$ associated with the switching of heteroatomic Ge$-$S covalent bonds into homoatomic S$-$S bonds are identified with the high-resolution XPS technique. The observed decrease in the concentration of lp-electrons on the valence-band spectrum for γ-irradiated sample is the most significant evidence for overcoordinated states of S atoms within the $Ge_3^-$$-$$S_3^+$ defect pairs. High-energy irradiation introduces two extra components within the S 2p spectrum, associated with S_3^+ defect atoms and irregular 2-fold coordinated S atoms within homoatomic S$-$S bonds. Additional components related to Ge 3d and Sb 4d peaks are linked with Ge_3^- defects and irregular 3-fold coordinated Sb atoms neighboring the S_3^+ defect, respectively.

Acknowledgment. We thank the National Science Foundation, through the International Materials Institute for New Functionality in Glass (IMI-NFG), for initiating and financially supporting our international collaboration (DMR-0409588).

References and Notes

(1) Shpotyuk, O. Radiation-induced effects in chalcogenide vitreous semiconductors. *Semiconducting Chalcogenide Glass 1*: *Glass Formation, Structure, and Simulated Transformations in Chalcogenide Glassess*; Fairman, R., Ushkov, B., Eds.; Elsevier Academic Press: New York, 2004; pp 215$-$260.

(2) Shpotyuk, O.; Matkovskii, A. *J. Non-Cryst. Solids* **1994**, *176*, 45.

(3) Kokenyesi, S.; Csikai, J.; Raics, P.; Szabo, I. A.; Szegedi, S.; Vitez, A. *J. Non-Cryst. Solids* **2003**, *326*$-$*327*, 209.

(4) Amin, G. A. M.; Spyrou, N. M. *Radiat. Phys. Chem.* **2005**, *72*, 419.

(5) Shpotyuk, O.; Balitska, V.; Vakiv, M.; Shpotyuk, L. *Sens. Actuators A*: *Phys.* **1998**, *68*, 356.

(6) Shpotyuk, O.; Golovchak, R.; Kavetskyy, T.; Kovalskiy, A. *Nucl. Instrum. Methods Phys. Res. B* **2000**, *166*$-$*167*, 517.

(7) Golovchak, R.; Shpotyuk, O. *Philos. Mag.* **2005**, *85*, 2847.

(8) Cohen, M.; Economou, E.; Soukoulis, C. *J. Non-Cryst. Solids* **1983**, *59*$-$*60*, 15.

(9) Antoine, K.; Jain, H.; Li, J.; Drabold, D. A.; Vlcek, M.; Miller, A. C. *J. Non-Cryst. Solids* **2004**, *349*, 162.

(10) Jain, H.; Krishnaswami, S.; Miller, A. C.; Krecmer, P.; Elliott, S. R.; Vlcek, M. *J. Non-Cryst. Solids* **2000**, *274*, 115.

(11) Li J.; Drabold, D. A.; Krishnaswami, S.; Chen, G.; Jain H. *Phys. Rev. Lett.* **2002**, *88*, 046803$-$1.

(12) Shpotyuk, O.; Kovalskiy, A.; Kavetskyy, T.; Golovchak, R. *J. Non-Cryst. Solids* **2005**, *351*, 993.

(13) Conny, J. M.; Powell, C. J. *Surf. Interface Anal.* **2000**, *29*, 856.

(14) Shpotyuk, O. *Phys. Status Solidi A* **1994**, *145*, 69.

(15) Dow, J. D.; Redfield, D. *Phys. Rev. B* **1970**, *1*, 3358.

(16) Tanaka, Ke. *J. Optoelectron. Adv. Mater.* **2001**, *3*, 189.

(17) Blaineau, S.; Jund, P. *Phys. Rev. B* **2004**, *70*, 184210.

(18) Foix, D.; Gonbeau, D.; Granier, D.; Pradel, A.; Ribes, M. *Solid State Ionics* **2002**, *154*$-$*155*, 161.

(19) Bergignat, E.; Hollinger, G.; Chermette, H.; Pertosa, P.; Lopez, D.; Lannoo, M.; Bensoussan, M. *Phys. Rev. B* **1988**, *37*, 4506.

(20) Lippens, P. E.; Olivier-Fourcade, J.; Jumas, J. C.; Gheorgiu, A.; Dupond, S.; Senemaud, C. *Phys. Rev. B* **1997**, *56*, 13054.

(21) Blaineau, S.; Jund, P.; Drabold, D. A. *Phys. Rev. B* **2003**, *67*, 94204$-$1$-$6.

(22) Hachiya, K. *J. Non-Cryst. Solids* **2002**, *312*$-$*314*, 566.

(23) Biswas, P.; De Nyago Tafen; Drabold, D. A. *Phys. Rev. B* **2005**, *71*, 54204-1-5.

(24) Hachiya, K. *J. Non-Cryst. Solids* **2001**, *291*, 160.

(25) Gheorghiu, A.; Lampre, I.; Dupont, S.; Senemaud, C.; El-Idrissi Raghni, M. A.; Lippens, P. E.; Olivier-Fourcade, J. *J. Alloys Compd.* **1995**, *228*, 143.

(26) Foix, D.; Martinez, H.; Gonbeau, D.; Pradel, A.; Ribes, M. *Chem. Phys.* **2005**, *7*, 180.

(27) Pauling, L. *The nature of the chemical bond*; Cornell University Press: Ithaca, NY, 1960; p 664.

(28) Debnath, R. K.; Fitzgerald, A. G.; Christova, K. *Appl. Surf. Sci.* **2002**, *202*, 261.

(29) Liudi Jiang; Fitzgerald, A. G.; Rose, M. J.; Christova, K.; Pamukchieva, V. *J. Non-Cryst. Solids* **2002**, *297*, 13.

(30) Debnath, R. K.; Fitzgerald, A. G.; Christova, K.; Manov, A. *J. Optoelectron. Adv. Mater.* **2005**, *7*, 353.